Synthesis of Aragonite from Precipitated Calcium Carbonate: A Pilot Scale Study

Ellyta Sari[1], Reni Desmiarti[1], Zulhadjri Zulhadjri[2], Matlal Fajri Alif[2], Maulana Yusup Rosadi[3], and Syukri Arief[2*]

[1]*Department of Chemical Engineering, Faculty of Industrial Technology, Universitas Bung Hatta, Jl. Gajah Mada No. 19, Padang 25173, Indonesia*

[2]*Department of Chemistry, Faculty of Mathematics and Natural Sciences, Universitas Andalas, Limau Manis Campus, Padang 25163, Indonesia*

[3]*Department of Civil Engineering, Faculty of Engineering, Universitas Borobudur, Jl. Kali Malang No. 1, Jakarta 13620, Indonesia*

* ***Corresponding author:***

email: syukriarief@sci.unand.ac.id

Received: December 19, 2023
Accepted: June 5, 2024

DOI: 10.22146/ijc.92169

Abstract: *The CO_2 mineralization pathway is considered a promising option for carbon capture usage and storage because the captured CO_2 can be permanently stored, and secondly industrial waste (i.e., petrochemical refinery, lime, and cement kiln dust) can be recycled into value-added carbonate materials by controlling the crystal polymorphs and properties of mineral carbonate. This study investigated the CO_2 mineralization utilized for the synthesis of precipitated calcium carbonate (PCC) via low temperatures at 30 °C and 55 °C with the addition of 50 and 75 g/L of ammonium chloride (NH_4Cl). The pilot scale of PCC production was established to simultaneously produce PCC with low energy demand by reporting the feasibility of economic analysis and to develop the mineral carbonation that can transform limestones and CO_2, which was captured from the petrochemical refinery process into economically valuable PCC. It is found that the aragonite phase of PCC can be generated at a room temperature of 30 °C by adjusting the CO_2 flow rate. In addition, the use of NH_4Cl, which transformed into ammonium carbonate ($(NH_4)_2CO_3$) during the calcination process, can maintain the stable aragonite phase by varying the NH_4Cl concentration.*

Keywords: *aragonite; carbon capture; CO_2 mineralization; precipitated calcium carbonate*

■ INTRODUCTION

Carbon dioxide (CO_2) mineralization has been proposed as a possible technique for CO_2 sequestration that enables permanent CO_2 storage without needing capture, storage location, transit pipes, or leakage monitoring [1]. Industries emit thousands of tons of CO_2 by manufacturing steel, iron, and non-metallic minerals such as cement and precipitated calcium carbonate (PCC). A strategy to remove CO_2 emissions is required to achieve a sustainable climate and environmental future. Carbon mineralization has been proposed to convert CO_2 into organic carbonates by utilizing natural mineral resources and industrial residues [2-6]. Recent strategies have demonstrated that CO_2 can be converted into high-purity PCC through carbon mineralization by elevating the temperature and high-purity CO_2 [7-9]. Synthesis of PCC from calcium oxide (CaO) also known as limestone is a highly potent technique and is used in a broad range of industries for several applications [2]. However, carbon mineralization has several limitations and problems that must be solved, including scalability, large-scale material consumption, and energy intensiveness. To tackle these problems, researchers have conducted many investigations in recent years, resulting in the publication of several advanced process approaches [10-13]. It is critical to have the pilot scale experiment to test the techno-economic feasibility of the technology during the transition from laboratory to industrial scale. CO_2 may be converted to mineral

carbonates by interacting with alkaline minerals found in geological formations, a process known as in situ mineral carbonation. Because mineral carbonates, such as $CaCO_3$ or $MgCO_3$, are the most thermodynamically stable form of carbon, long-term storage of CO_2 is possible when it is converted to carbonates.

$CaCO_3$ is a common mineral in nature, accounting for around 5% of the Earth's crust in the forms of limestone, chalk, and marble. $CaCO_3$ is used as a filler or coating pigment in paper, plastics, rubbers, and adhesives; as a filler, extender, and pH buffer in paints; as a filler and color stabilizer in concrete [14]; for environmental pollution control and remediation in flue gas and water treatment [15-16]; as a calcium source in fertilizers and animal feed [17]; and in glass, ceramics, cosmetics, and hygiene [18-19]. High purity $CaCO_3$, known as PPC exhibits different crystalline polymorphs at ambient pressure: calcite, aragonite, and vaterite. Synthetic variables such as pH, temperature, concentration, and the ratio of carbonate and calcium ions, additives, stirring, reaction duration, and others have been documented to impact the formation behavior of each polymorph [20-21]. Calcite is a simple material to manufacture since it is the thermodynamically stable phase at room temperature and pressure, vaterite is an unstable phase, whereas aragonite is a metastable phase. Aragonite has the highest aspect ratio of these polymorphs and is considered a novel functional inorganic particle capable of altering the mechanical and optical characteristics of rubber, plastics, paints, and varnishes as a filler. As a pigment, it may also increase the strength and brightness of paper, as well as modify its opacity. Aragonite is the stable phase only below 75 K at atmospheric pressure [22]. However, the production of aragonite phase PCC is known to be extremely difficult since the aragonite phase can rapidly convert into thermodynamically stable calcite [23]. Thus, the management of maintaining the produced aragonite phase PCC is required by utilizing the effective amount of CO_2.

Numerous studies have demonstrated that CO_2 mineralization synthesizes economically valuable PCC using industrial waste as raw materials with low energy demand. Previous studies compared the nucleation and crystal development rates of calcite and aragonite from supersaturated fluids to examine the effect of temperature on aragonite formation [24-25]. Ren et al. [26] demonstrated that 1 mol/L NaCl solution could improve the leaching rate of Ca^{2+} by mineralizing 280 kg CO_2/t-slag. PCC production utilizing CO_2 within temperatures ranging from 25 to 55 °C was observed by Samanta et al. [2], whereas a high temperature of 55 °C produced a needle-like aragonite phase. PCC was prepared by adding ammonium carbonate to the distillation waste stream, and the filtrate can be distilled to obtain high-purity ammonium chloride (NH_4Cl), which is widely used in fertilizer, food, and other fields [27]. However, factors such as limited solubility of $Ca(OH)_2$ due to a long reaction time in aqueous media affect the ways of processing PCC. In some cases, processing PCC took a long time and produced a small amount of $CaCO_3$ due to limited soluble $Ca(OH)_2$ in aqueous media [28-29]. Moreover, the formation of aragonite PCC requires a high temperature at a low pH solution to manage the stability of produced aragonite, which can increase the energy demand for the carbonation process. In a study by [30], aragonite formed at a temperature of 80 °C and might transform into calcite when the temperature increased to 100 °C. Despite the success of the formation of calcite, the stability of aragonite crystal should be managed to meet the demand for products with low energy demand. The stability of aragonite PCC is also affected by the additives used in the making of PCC, such as amino acids, surfactants, protein, sugar, and inorganic ions [31]. However, there is still a gap in the clear understanding of the low temperature and the additives controlling the physical and chemical properties of aragonite PCC. This work presents the exploration and the information of the low temperature and NH_4Cl as the additive via CO_2 mineralization affected the formation of aragonite PCC. In this study, we synthesized the aragonite phase at low temperatures of 30 °C and 50 °C. A pilot scale of the PCC synthesis was done by utilizing CO_2 mineralization in aqueous media in the presence of ammonium carbonate ($(NH_4)_2CO_3$), which was obtained by varying the starting materials of NH_4Cl at the concentrations of 50 and 75 g/L. This study aims to synthesize new aragonite PCC

at lower reaction temperatures than existing synthetic techniques by using a combination of NH_4Cl salts and CO_2 gas, thereby improving the economic value of aragonite PCC.

■ EXPERIMENTAL SECTION

Materials

Natural quicklime was obtained from a karst in Padalarang, West Java, Indonesia, and its characteristics are shown in Table 1.

Instrumentation

The chemical compositions of the raw limestone were analyzed using an X-ray fluorescence (XRF) spectrometer (Malvern Panalytical, Worcestershire, United Kingdom). Detailed information about the XRF analysis: samples are crushed and pulverized according to default preparation procedures. Sample preparation entails the formation of a homogenous glass disk by the fusion of the sample and a lithium tetraborate mixture. The loss on ignition (LOI) is determined separately and gravimetrically at 1000 °C. The prepared disks are analyzed by wavelength dispersion XRF (WD-XRF). The LOI is included in the matrix correction calculation, which is performed by the XRF software. The crystalline phases of the powders and their products were analyzed using X-ray diffraction (XRD) analysis (Empyream diffractometer, Malvern Panalytical, Worcestershire, United Kingdom) with Cu Kα radiation (40 kV, 25 mA). The samples were scanned over the 2θ from 10° to 90°. The particle size distributions of the materials were determined using an LA-960v2 particle size analyzer (Horiba, Tokyo, Japan). The particle morphologies before and after the reaction were determined using scanning electron microscopy (SEM) (Quanta FEG 450, FEI, Tokyo, Japan). The FTIR was carried out in the 3750–750 cm^{-1} range using Irprestige-21 (Shimadzu, Tokyo, Japan).

Table 1. Characteristics of quicklime used for PCC synthesis

Chemical composition	Percentage (%)
CaO	86.95
MgO	0.50
Cl	11.26
SO_4	1.31
SiO_2	0.12

Procedure

Formation of calcium chloride ($CaCl_2$) and ammonium hydroxide (NH_4OH)

The modifications were made to the slaking process. The dissolution of calcined limestone is dissolved in a solution containing water ions and NH_4Cl salt. It is expected that by adding salt, more calcium will be formed. Fig. 1 shows the design of the pilot plant for PCC production. The plant consists of a continuous stirred tank reactor (CSTR) and a plug flow bubble reactor (PFBR). The PCC synthesis process begins with the production of $CaCl_2$ and NH_4OH utilizing a CSTR to react with CaO in a CaO tank with NH_4Cl solution in an NH_4Cl tank using a CSTR. CaO:NH_4Cl:H_2O has a stoichiometric mole ratio of 1:2.5:1000. The CaO utilized as a raw material has a purity of 95–98%, while the technical NH_4Cl has a purity of 98%. The reactions are shown in Eq. (1) and (2).

$$2CaO_{(2)}+4NH_4Cl_{(aq)}+H_2O_{(l)}\rightarrow 2CaCl_{2(aq)}+3NH_4OH_{(aq)}+NH_{3(g)} \quad (1)$$

$$CaO_{(s)}+H_2O_{(l)}\rightarrow Ca(OH)_{2(s)} \quad (2)$$

The CSTR reactor was stirred for 1 h at a temperature of 30 °C. $CaCl_2$ and NH_4OH are produced as byproducts of this reaction, while impurities present in limestone that are not dissolved are separated as raw material for subsequent reactions using a vacuum filter. Meanwhile, the produced NH_3 gas will be returned to the NH_4Cl tank. After that, the NH_4OH is injected into the PFBR. $CaCO_3$ formation happens in three phases of the process.

CO_2 absorption and mineralization

The CO_2 gas flows into the filtrate, resulting in a white PCC precipitation, and releases back NH_4Cl into the solution. With this system, the synthesis procedure can be done repeatedly with a continuous system. The pilot plant can handle up to 10 L/min of CO_2 gas and 60 L of liquid solvent in batch mode, and it can generate around 2 kg of PCC/h. The chemical solvent may be collected and reused in the calcium extraction stage after carbonation, making the process more economically viable.

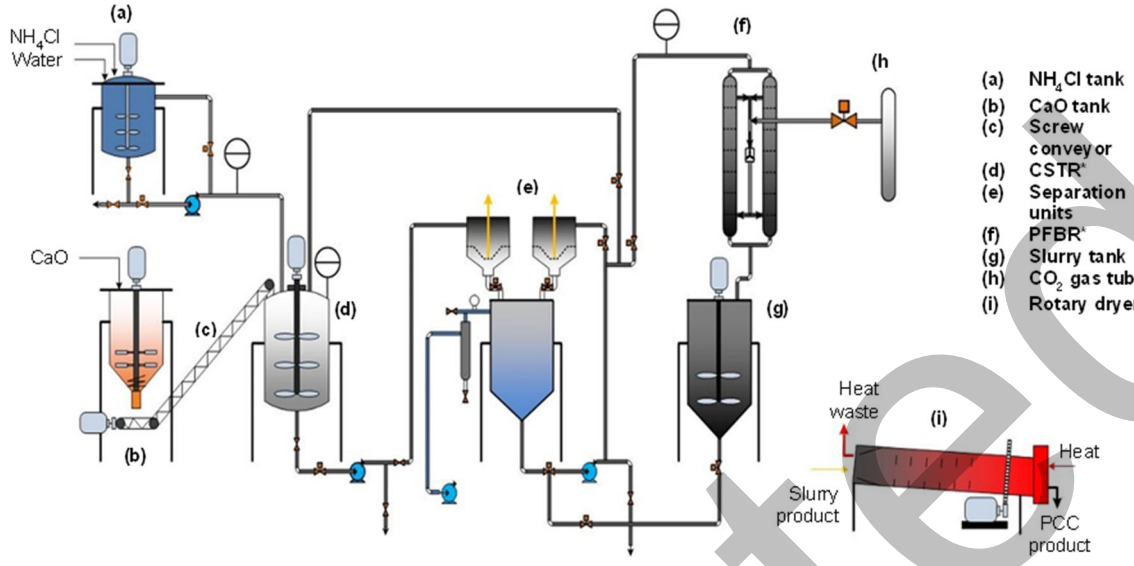

Fig 1. PCC pilot scale using PFBR reactor to produce aragonite phase PCC

$(NH_4)_2CO_3$ is produced by reacting NH_4OH with CO_2. The following process shows the chemical synthesis of $(NH_4)_2CO_3$ with a conversion rate of 100%, in which NH_4OH is completely reacted with CO_2 to form $(NH_4)_2CO_3$ (Eq. 3).

$$2NH_4OH_{(aq)}+CO_{2(g)}\rightarrow(NH_4)_2CO_{3(aq)}+H_2O_{(l)} \quad (3)$$

Reacting the $(NH_4)_2CO_3$ with $CaCl_2$ to produce $CaCO_3$, can be explained in Eq. (4).

$$(NH_4)_2CO_{3(aq)}+CaCl_{2(aq)}\rightarrow CaCO_{3(s)}+2NH_4Cl_{(aq)} \quad (4)$$

$Ca(OH)_2$ is reacted with CO_2 gas to produce $CaCO_3$ as shown in Eq. (5).

$$Ca(OH)_{2(s)}+CO_{2(g)}\rightarrow CaCO_{3(s)}+H_2O_{(l)} \quad (5)$$

At room temperature and pressure, the process to produce $CaCO_3$ lasted 1 h. The $CaCO_3$ produced is subsequently removed from the NH_4Cl solution using a vacuum filter and returned to the CSTR as raw material. A rotary dryer is used to dry the product at temperatures ranging from 70 to 90 °C. This system also includes transportation equipment like screw conveyors for CaO transfer and pumps for fluid transport.

RESULTS AND DISCUSSION

Chemical Composition of Limestone

The chemical compositions of limestone used in this study and the changes in its compositions after mineralization are shown in Table 2. It is observed that CO_2 mineralization increased the composition of $CaCO_3$ and lowered the composition of Cl. The temperature of 50 °C with 75 g/L NH_4Cl caused an increase in the content of $CaCO_3$ by 8%. This suggested that high temperatures

Table 2. Chemical compositions of raw limestone and the produced $CaCO_3$ after CO_2 mineralization

Chemical composition	Chemical compositions			
	NH_4Cl 75 g/L (55 °C)	NH_4Cl 75 g/L (30 °C)	NH_4Cl 50 g/L (55 °C)	NH_4Cl 50 g/L (30 °C)
$CaCO_3$	94.97	87.50	92.67	97.40
Cl	3.72	11.87	5.32	1.15
SO_4	0.90	0.37	1.28	0.88
SiO_2	0.11	0.10	0.22	0.19
MgO	0.07	< 0.02	0.18	0.13
Al_2O_3	0.07	0.05	0.13	0.09
SrO	0.04	0.03	0.04	0.03
P_2O_5	< 0.02	< 0.02	0.02	< 0.02

increase the decomposition rate of CaO. At the same time, CO_2 mineralization could promote the high protonation reaction between the produced $(NH_4)_2CO_3$, increasing the Ca conversion rate [32]. However, $CaCO_3$ was the highest when NH_4Cl concentration was 50 g/L and at the temperature of 30 °C, while 75 g/L NH_4Cl at 30 °C produced the lowest $CaCO_3$. The condition of NH_4Cl 50 g/L suggested the good immobilization of NH_4Cl into the solid particle, thus increasing the extraction efficiency. The excess of NH_4Cl might stop the advancement of the reaction of Ca-rich solution with CO_2 to form PCC. The finding affirmed the high concentration of NH_4Cl can extract impurities, such as Cl, S, Mg, and Mn, due to higher molarity against the larger particle size [33], thus limiting the Ca extraction efficiency.

Morphology of Produced PCC by SEM Images

The SEM pictures of the aragonite samples are shown in Fig. 2. The Ca-rich solution from the extraction stage was reacted with CO_2 gas in a carbonation reactor, resulting in PCC production. The quality of PCC was critical to the technology's economic success. Calcite, aragonite, and vaterite are the three anhydrous crystallizes of $CaCO_3$ produced in order of stability. The most critical parameter in determining the crystal shape of the PCC was found to be the initial carbonation temperature [22]. Aragonite PCC is generated at higher temperatures (> 55 °C) in traditional PCC procedures [34-35], but not in this proposed technique. This study achieved synthesized aragonite at a relatively low temperature (40–50 °C).

At a high gas flow rate, i.e., 10 L/min, the particles resulted in the calcite and aragonite shape which formation was favored by the prevalence of Ca^{2+} over CO_3^{2-} [36]. Aragonite particles were characterized by needle-shape appearance when viewed in SEM, while calcite particles were often identified by rhombohedral crystal shapes. The morphology transition from calcite to aragonite particles can be explained by the gradual increase in the pH of the solution. By this, this study observed that aragonite particles were formed at H values slightly lower than 12, while calcite particles could be formed at pH values lower than 11 [32]. The temperature of 55 °C with 75 g/L NH_4Cl showed almost a single aragonite crystal type, while the other conditions showed a mixture of aragonite and calcite particles, but they were identified as clusters of spherical particles that could be a vaterite crystal growth. PCC particles formed at 30 °C have a similar particle size distribution to the particles formed at 55 °C (Table 3). This could be because the reduction of

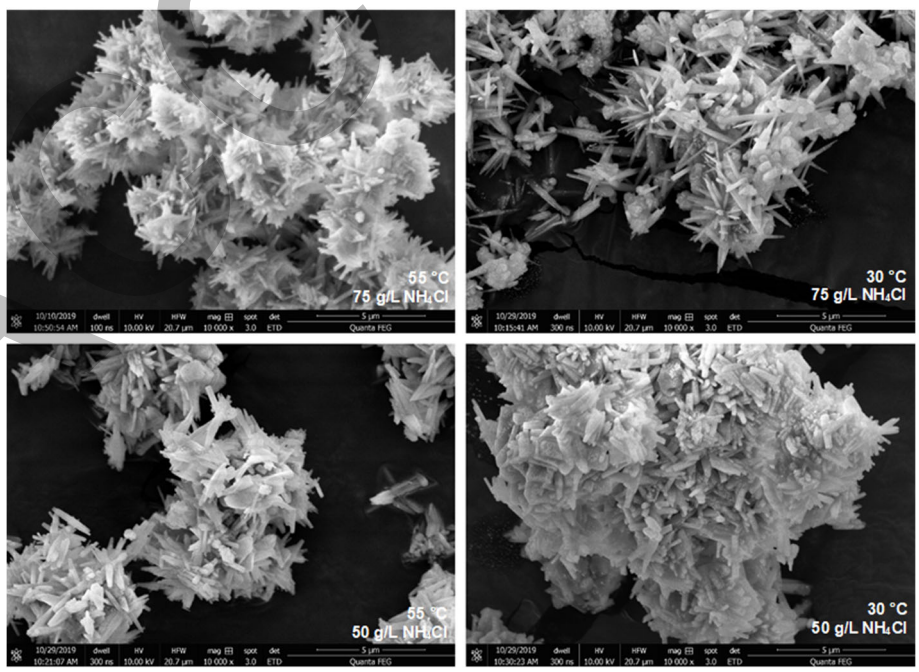

Fig 2. SEM images of synthesized PCC under different reaction temperatures and NH_4Cl concentrations

Table 3. Effect of low temperatures on the particle size distribution of PCC

Particle diameter (nm)	Number distribution (%)				
		Sample conditions			
	Raw limestone	NH_4Cl 75 g/L (55 °C)	NH_4Cl 75 g/L (30 °C)	NH_4Cl 50 g/L (55 °C)	NH_4Cl 50 g/L (30 °C)
0.5	1.0	6.0	3.5	1.9	0.2
1.0	3.4	15.8	10.8	5.6	3.1
5.0	16.5	48.1	45.9	29.2	61.7
12.0	28.8	80.8	75.7	59.4	87.7
15.0	39.7	93.9	91.4	81.6	94.4
20.0	46.2	96.5	95.9	95.5	98.3
30.0	59.5	97.6	99.0	99.5	99.7
40.0	65.8	97.7	99.3	99.7	99.9
60.0	74.5	97.7	99.8	99.8	99.9
75.0	79.2	97.7	99.9	100.0	99.9
100.0	83.9	97.7	100.0	100.0	100.0
160.0	87.6	98.7	100.0	100.0	100.0
200.0	89.2	99.4	100.0	100.0	100.0
300.0	91.1	100.0	100.0	100.0	100.0

the nucleation rate was not significantly changed by the increase in temperature. However, the cluster of aragonite particles observed by SEM demonstrated the subsequent nucleation of calcite into aragonite.

Particle size analyses of PCC products showed that the particle size above 20 nm increased in their number distribution (Table 3). Temperature plays an essential role in PCC crystal formation to control the solubility and activity of Ca^{2+} and CO_3^{2-} ions [37]. The increase in temperature might promote the crystal growth during the carbonation to form clusters of greater size. A previous finding reported the acceleration of the agglomeration of nanoparticles when the temperature was increased [38]. The study showed that the temperature of 60 resulted in a larger particle with a diameter of 225 nm compared to the temperature of 40 °C. However, our findings showed that low temperatures of 30 °C can promote the particle number distribution and form the large particle size up to 300 nm. This confirmed that the crystallization could occur with early-stage nucleation assisted by additives. Moreover, in the condition at the high concentration of NH_4Cl at 55 °C, the number distribution at 100 nm is lower compared to the other conditions. When considering the mechanisms underlying $CaCO_3$ formation, the effect of surface energy on the particle formation is not negligible. Surface energy on the large particle is lower compared to the small particle due to the negative charge development at the $CaCO_3$ surface [39]. With the addition of a high concentration of NH_4Cl, the small solid particles and the more associated solute diffuse through the liquid and the re-precipitates take a longer time to form larger particles [3].

Morphology of Produced PCC by XRD and FTIR

Fig. 3 shows the XRD patterns of PCC with the effect of the addition of NH_4Cl at the concentrations of 75 and 50 g/L. All samples showed the presence of calcite and aragonite at low temperatures. This finding was consistent with the previous work by Kajiyama et al. [40] and Ramakrishna et al. [41] that aragonite phase PCC could be synthesized above room temperature in the range of 30–55 °C. The temperature is crucial to ensure the formation of the aragonite phase in the composite polymorph, which increases the net energy required for this phase. Hence, this phenomenon is unattractive from an industrial standpoint. In addition, 50 and 75 g/L of NH_4Cl, $(NH_4)_2CO_3$ was produced and promoted the calcite and aragonite crystals. However, as shown in Fig. 3, at the temperature of 55 °C, calcite was the only carbonate species detected by XRD under the addition effect of 75 g/L NH_4Cl.

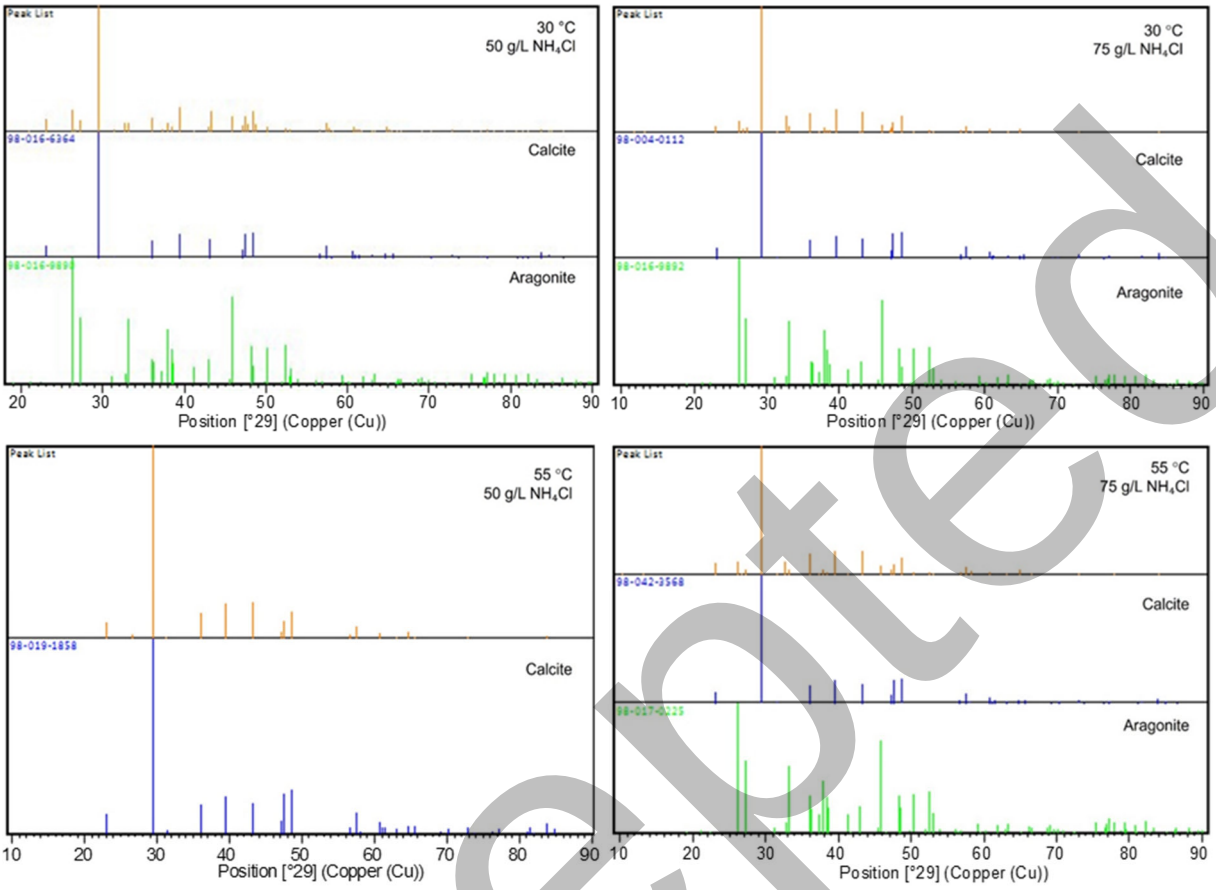

Fig 3. XRD patterns of PCC synthesized at different temperatures and NH_4Cl concentrations

A previous study mentioned that $(NH_4)_2CO_3$ could promote the calcite-vaterite and calcite-aragonite polymorph formation at 30–70 °C [42]. However, a study by Yoo et al. [43] demonstrated that aragonite formed under high temperature and low pH conditions. In this study, the pH during the carbonation process was at alkaline pH ranging between 12 and 13, so we assume that pH is so high that morphology control is partially lost. In addition, the $(NH_4)_2CO_3$ can influence the behavior of $CaCO_3$ crystallization by modifying the surface energy at the interface between the solvent and $CaCO_3$ crystals [36]. This can conclude the absence of aragonite crystals at 50 °C. Another reason could be that the complexation of Ca^{2+} ions by $(NH_4)_2CO_3$ increased the CO_3^{2-}/Ca^{2+} ratio thus favoring the formation of calcite over aragonite [44]. In other words, the effect of NH_4Cl creates an environment that promotes the formation of either aragonite crystals or calcite crystals. This study showed that the reaction $(NH_4)_2CO_3$ and $CaCl_2$ resulted in a low ratio of CO_3^{2-}/Ca^{2+} and was less affected by temperature. To some extent, higher Ca^{2+} ion concentration is conducive to the formation of calcite.

Table 4 shows the FTIR peak vibrants of the PCC obtained from the low temperature of CO_2 mineralization and their patterns are available in Fig. S1. After 1 h of reaction, the sample exhibited the characteristic absorption peaks of calcite at around 850–880 cm^{-1}. The temperature of 55 °C with the effect of 50 g/L NH_4Cl causes the stretching of CO_3^{2-} groups of $CaCO_3$ and 1084 cm^{-1}, showing the absorption peak of aragonite crystals. In addition, C–H stretching (2830–2980 cm^{-1}) and the O–H stretching (3420 cm^{-1}) of obtained PCC were observed, indicating that the reaction mechanisms involving the NH_4Cl as the washing agent coordinated with PCC during the carbonation process. When the initial CaO reacted with NH_4Cl to form NH_4OH, the mineralization of CO_2 took place to form $(NH_4)_2CO_3$, resulting in the occurrence of a

Table 4. FTIR peaks of PCC synthesized at different temperatures and NH_4Cl concentrations

Sample conditions							
NH_4Cl 50 g/L (30 °C)		NH_4Cl 50 g/L (55 °C)		NH_4Cl 75 g/L (30 °C)		NH_4Cl 75 g/L (55 °C)	
Peak (cm^{-1})	Intensity (%)	Peak (cm^{-1})	Intensity (%)	Peak (cm^{-1})	Intensity (%)	Peak (cm^{-1})	Intensity (%)
855	41	854	57	855	69	876	71
1082	86	955	84	953	96	1146	96
1456	51	1084	81	1082	95	1395	77
1647	92	1153	81	1159	96	1464	81
2359	97	1252	84	1260	96	2355	96
3402	84	1506	63	1516	75		
		2359	87	2357	92		
		2980	76	2980	91		

new absorption peak and the deformation band of CO_3^{2-} occurred, indicating the sample is aragonite phase $CaCO_3$ at 1082–1500 cm^{-1}. All the synthesis conditions lead to the formation of calcite and aragonite crystals, and the results are consistent with the XRD peak. When the concentration of NH_4Cl was 75 g/L and reacted under the temperature of 30 °C, the nucleation rate of $CaCO_3$ was slow and aragonite could not be formed in a short time. Another possibility was that the generated aragonite was reversely transformed into calcite by the process of dissolution and recrystallization because the reaction period was only 1 h.

Economic Analysis of the Pilot Plant of PCC Synthesis

The cost correlation method was used to estimate capital investment. The capital cost of the pilot plant, such as CSTR, PFBR, dryer, conveyor, etc., were estimated and the cost is shown in Table 5. The total capital investment of PCC production is about US$ 35,240,828. The total production cost is US$ 21,697,371, which comes from the cost of raw materials, the cost of direct labor, and the cost of overhead. The depreciation period was assumed to be 10 years with an inflation rate of 2.50%/year, and an income tax rate of 12.50% was used. The pilot scale of PCC synthesis shall be subjected to a production capacity of 350 tons/day. The market price of PCC in Indonesia is US$ 0.44/kg, which was an average price from 2021 and 2022. The produced PCC from the pilot plant has a 20.00% price of the market price, US$ 0.35/kg. Therefore,

Table 5. Total capital investment of PCC production

Equipment	Unit	Cost in US$
CaO vessel	1	256,408
NH_4Cl vessel	1	491,218
Screw conveyor	1	5,068
CSTR	1	1,262,132
PFR	1	1,145,089
Storage tank	2	512,816
Separator	2	647,235
Rotary dryer	1	309,862
Centrifugal pump	6	318,549
Vacuum pump	2	141,417
Total cost		5,089,793
Total direct cost		21,251,158
Total indirect cost		4,786,950
Fixed capital investment		29,954,704
Working capital		4,493,206
Total capital investment		35,240,828

the annual sale of PCC is about US$ 33,26,992 at the start-up time of 2 years and increases by about US$ 36,959,992 after 3 years with 100% plant performance. Assuming 10 years of plant performance, the annual sales and total production cost could increase with the inflation rate, in which the average annual sales would be greater than the first year of performance. Return on investment (ROI) and payback period (PBP) are reported to be 37.90% and 3.60 years, respectively. The economic analysis showed that the plant could be feasible on its performance with a production capacity of 350 tons/day, which resulted in a 32.30% break event point.

■ CONCLUSION

This study investigated the performance of a pilot scale of PCC synthesis via CO_2 mineralization at low temperatures of 30 °C and 55 °C. NH_4Cl was used to obtain the $(NH_4)_2CO_3$ as a reacting agent to produce PCC. The process scale-up was a huge success; the pilot plant ran precisely as planned, and the findings were very encouraging. Aragonite phase PCC was produced at 30 °C by maintaining the CO_2 flow rate of 10 L/min. The spectroscopy analytical results of XRD, SEM, and FTIR confirmed the formation of aragonite phase PCC under low temperatures and varied NH_4Cl, which successfully enhanced the quality of PCC. The novel approach demonstrated in this work is to synthesize PCC cost-effectively by capturing the wasted CO_2 from the petrochemical refinery process, thus reducing the CO_2 emission to the environment. It was found that the PCC pilot plant has economic feasibility within 3.6 years of plant performance with the production of 350 tons/day.

■ ACKNOWLEDGMENTS

This work was supported by PT Pertamina (Persero) with grant number 001/P00000/2020-S0 and Research and Community Service Division Universitas Bung Hatta with grant number 008/LPPM-Penelitian/Hatta/III-2024. The authors would like to thank all the technical staff from PT Pertamina (Persero) for their assistance in this work.

■ CONFLICT OF INTEREST

The authors declare that they have no known competing financial interests or personal relationships that could have appeared to influence the work reported in this paper.

■ AUTHOR CONTRIBUTIONS

Ellyta Sari: Conceptualization, methodology, investigation, resources, data curation, writing, review and editing; Reni Desmiarti, Zulhadjri, Matlal Fajri Alif, Maulana Yusup Rosadi: Conceptualization, methodology, formal analysis, data curation, writing draft preparation; Syukri Arief: Validation, writing, review and editing, data curation, supervision; All authors have read and agreed to the published version of the manuscript.

■ REFERENCES

[1] Krishnan, A., Nighojkar, A., and Kandasubramanian, B., 2023, Emerging towards zero carbon footprint via carbon dioxide capturing and sequestration, *Carbon Capture Sci. Technol.*, 9, 100137.

[2] Samanta, N.S., Anweshan, A., Mondal, P., Bora, U., and Purkait, M.K., 2023, Synthesis of precipitated calcium carbonate from LD-slag using CO_2, *Mater. Today Commun.*, 36, 106588.

[3] Yin, T., Yin, S., Srivastava, A., and Gadikota, G., 2022, Regenerable solvents mediate accelerated low temperature CO_2 capture and carbon mineralization of ash and nano-scale calcium carbonate formation, *Resour., Conserv. Recycl.*, 180, 106209.

[4] Gadikota, G., 2021, Carbon mineralization pathways for carbon capture, storage and utilization, *Commun. Chem.*, 4 (1), 23.

[5] Ji, L., Yu, H., Zhang, R., French, D., Grigore, M., Yu, B., Wang, X., Yu, J., and Zhao, S., 2019, Effects of fly ash properties on carbonation efficiency in CO_2 mineralisation, *Fuel Process. Technol.*, 188, 79–88.

[6] Ding, W., Fu, L., Ouyang, J., and Yang, H., 2014, CO_2 mineral sequestration by wollastonite carbonation, *Phys. Chem. Miner.*, 41 (7), 489–496.

[7] Tan, W.L., Tan, H.F., Ahmad, A.L., and Leo, C.P., 2021, Carbon dioxide conversion into calcium carbonate nanoparticles using membrane gas absorption, *J. CO_2 Util.*, 48, 101533.

[8] Hong, S., Sim, G., Moon, S., and Park, Y., 2020, Low-temperature regeneration of amines integrated with production of structure-controlled calcium carbonates for combined CO_2 capture and utilization, *Energy Fuels*, 34 (3), 3532–3539.

[9] Liu, M., and Gadikota, G., 2020, Single-step, low temperature and integrated CO_2 capture and conversion using sodium glycinate to produce calcium carbonate, *Fuel*, 275, 117887.

[10] Alturki, A., 2022, The global carbon footprint and how new carbon mineralization technologies can be used to reduce CO_2 emissions, *ChemEngineering*, 6 (3), 44.

[11] Kelemen, P.B., McQueen, N., Wilcox, J., Renforth, P., Dipple, G., and Vankeuren, A.P., 2020, Engineered carbon mineralization in ultramafic rocks for CO_2 removal from air: Review and new insights, *Chem. Geol.*, 550, 119628.

[12] de Oliveira Costa Souza Rosa, C., da Silva Christo, E., Costa, K.A., and dos Santos, L., 2020, Assessing complementarity and optimizing the combination of intermittent renewable energy sources using ground measurements, *J. Cleaner Prod.*, 258, 120946.

[13] Mohd Pauzi, M.M., Azmi, N., and Lau, K.K., 2022, Emerging solvent regeneration technologies for CO_2 capture through offshore natural gas purification processes, *Sustainability*, 14 (7), 4350.

[14] Ye, J., Liu, S., Fang, J., Zhang, H., Zhu, J., and Guan, X., 2023, Synthesis of aragonite whiskers by co-carbonation of waste magnesia slag and magnesium sulfate: Enhancing microstructure and mechanical properties of Portland cement paste, *Buildings*, 13 (11), 2888.

[15] Zhai, M., Guo, L., Sun, L., Zhang, Y., Dong, P., and Shi, W., 2016, Desulfurization performance of fly ash and $CaCO_3$ compound absorbent, *Powder Technol.*, 305, 553–561.

[16] de Beer, M., Maree, J.P., Liebenberg, L., and Doucet, F.J., 2014, Conversion of calcium sulphide to calcium carbonate during the process of recovery of elemental sulphur from gypsum waste, *Waste Manage.*, 34 (11), 2373–2381.

[17] Ozyhar, T., Marchi, M., Facciotto, G., Bergante, S., and Luster, J., 2022, Combined application of calcium carbonate and NPKS fertilizer improves early-stage growth of poplar in acid soils, *For. Ecol. Manage.*, 514, 120211.

[18] Carella, F., Degli Esposti, L., Adamiano, A., and Iafisco, M., 2021, The use of calcium phosphates in cosmetics, state of the art and future perspective, *Materials*, 14 (21), 6398.

[19] Saulat, H., Cao, M., Khan, M.M., Khan, M., Khan, M.M., and Rehman, A., 2020, Preparation and applications of calcium carbonate whisker with a special focus on construction materials, *Constr. Build. Mater.*, 236, 117613.

[20] Kogo, M., Umegaki, T., and Kojima, Y., 2019, Effect of pH on formation of single-phase vaterite, *J. Cryst. Growth*, 517, 35–38.

[21] Hu, Y.B., Wolthers, M., Wolf-Gladrow, D.A., and Nehrkle, G., 2015, Effect of pH and phosphate on calcium carbonate polymorphs precipitated at near-freezing temperature, *Cryst. Growth Des.*, 15 (4), 1596–1601.

[22] Altiner, M., and Yildirim, M., 2017, Production and characterization of synthetic aragonite prepared from dolomite by eco-friendly leaching-carbonation process, *Adv. Powder Technol.*, 28 (2), 553–564.

[23] Liendo, F., Arduino, M., Deorsola, F.A., and Bensaid, S., 2022, Factors controlling and influencing polymorphism, morphology and size of calcium carbonate synthesized through carbonation route: A review, *Powder Technol.*, 398, 117050.

[24] Eichinger, S., Boch, R., Baldermann, A., Goetschl, K., Wenighofer, R., Hoffmann, R., Stamm, F., Hippler, D., Grengg, C., Immenhauser, A., and Dietzel, M., 2023, Unraveling calcite-to-aragonite evolution from a subsurface fluid – Formation pathway, interfacial reactions and nucleation effects, *Chem. Geol.*, 641, 121768.

[25] Bergwerff, L., and van Paassen, L.A., 2021, Review and recalculation of growth and nucleation kinetics for calcite, vaterite and amorphous calcium carbonate, *Crystals*, 11 (11), 1318.

[26] Ren, E., Tang, S., Liu, C., Yue, H., Li, C., and Liang, B., 2018, Carbon dioxide mineralization for the disposition of blast-furnace slug: Reaction intensification using NaCl solutions, *Greenhouse Gases: Sci. Technol.*, 10 (2), 436–448.

[27] Asakai, T., Suzuki, T., Miura, T., and Hioki, A., 2014, Certified reference material for ammonium ions in high-purity ammonium chloride: Influence of pH on coulometric titration of ammonium ions with electrogenerated hypobromite, *Microchem. J.*, 114, 203–209.

[28] Arifin, Z., Zainuri, M., Cahyono, Y., and Darminto, D., 2018, The influence of temperature and gas flow rate on the formation $CaCO_3$ vaterite phase, *IOP Conf. Ser.: Mater. Sci. Eng.*, 395 (1), 012004.

[29] Shirsath, S.R., Sonawane, S.H., Saini, D.R., and Pandit, A.B., 2015, Continuous precipitation of calcium carbonate using sonochemical reactor, *Ultrason. Sonochem.*, 24, 132–139.

[30] Tone, T., and Koga, N., 2023, Interplay between thermally induced aragonite-calcite transformation and multistep dehydration in a seawater spiral shell (*Euplica scripta*), *Processes*, 11 (6), 1650.

[31] Jimoh, O.A., Okoye, P.U., Otitoju, T.A., and Ariffin, K.S., 2018, Aragonite precipitated calcium carbonate from magnesium rich carbonate rock for polyethersulfone hollow fibre membrane application, *J. Cleaner Prod.*, 195, 79–92.

[32] Marin Rivera, R., and Van Gerven, T., 2020, Production of calcium carbonate with different morphology by simultaneous CO_2 capture and mineralization, *J. CO_2 Util.*, 41, 101241.

[33] Wang, J., Li, Z., Park, A.H.A., and Petit, C., 2015, Thermodynamic and kinetic studies of the $MgCl_2$-NH_4Cl-NH_3-H_2O system for the production of high purity MgO from calcined low-grade magnesite, *AIChE J.*, 61 (6), 1933–1946.

[34] Mei, X., Zhao, Q., Li, Y., Min, Y., Liu, C., Saxen, H., and Zevenhoven, R., 2022, Phase transition and morphology of precipitated calcium carbonate (PCC) in the CO_2 mineralization process, *Fuel*, 328, 125259.

[35] Lu, H., Huang, Y.C., Hunger, J., Gebauer, D., Cölfen, H., and Bonn, M., 2021, Role of water in $CaCO_3$ biomineralization, *J. Am. Chem. Soc.*, 143 (4), 1758–1762.

[36] Lu, J., Ruan, S., Liu, Y., Wang, T., Zeng, Q., and Yang, D., 2022, Morphological characteristics of calcium carbonate crystallization in CO_2 pre-cured aerated concrete, *RSC Adv.*, 12 (23), 14610–14620.

[37] Grimes, C.J., Hardcastle, T., Manga, M.S., Mahmud, T., and York, D.W., 2020, Calcium carbonate particle formation through precipitation in a stagnant bubble and a bubble column reaction, *Cryst. Growth Des.*, 20 (8), 5572–5582.

[38] Li, W., Huang, Y., Wang, T., Fang, M., and Li, Y., 2022, Preparation of calcium carbonate nanoparticles from waste carbide slag based on CO_2 mineralization, *J. Cleaner Prod.*, 363, 132463.

[39] Minkowicz, L., Dagan, A., Uvarov, V., and Benny, O., 2021, Controlling calcium carbonate particle morphology, size, and molecular order using silicate, *Materials*, 14 (13), 3525.

[40] Kajiyama, S., Nishimura, T., Sakamoto, T., and Kato, T., 2014, Aragonite nanorods in calcium carbonate/polymer hybrids formed through self-organization process from amorphous calcium carbonate solution, *Small*, 10 (8), 1634–1641.

[41] Ramakhrisna, C., Thenepalli, T., Huh, J.H., and Ahn, J.W., 2016, Preparation of needle like aragonite precipitated calcium carbonate (PCC) from dolomite by carbonation method, *J. Korean Ceram. Soc.*, 53 (1), 7–12.

[42] Luo, M., Zhang, G., Fang, Y., Cao, L., Guo, Z., Wang, K., and Li, J., 2023, Calcium carbonate crystallization process from the mineralization of calcium chloride waste, *Sep. Purif. Technol.*, 319, 124066.

[43] Yoo, Y., Kim, I., Lee, D., Yong Choi, W., Choi, J., Jang, K., Park, J., and Kang, D., 2022, Review of contemporary research on inorganic CO_2 utilization via CO_2 conversion metal carbonate-based materials, *J. Ind. Eng. Chem.*, 116, 60–74.

[44] Chang, R., Choi, D., Kim, M.H., and Park, Y., 2017, Tuning crystal polymorphisms and structural investigation of precipitated calcium carbonates for CO_2 mineralization, *ACS Sustainable Chem. Eng.*, 5 (1), 1659–1667.